

Copper Sintering Pastes with Various Polar Solvents and Acidic Activators

Seungyeon Lee,[§] Seong-ju Han,[§] Yongjune Kim, and Keon-Soo Jang*Cite This: *ACS Omega* 2023, 8, 39135–39142

Read Online

ACCESS |



Metrics & More

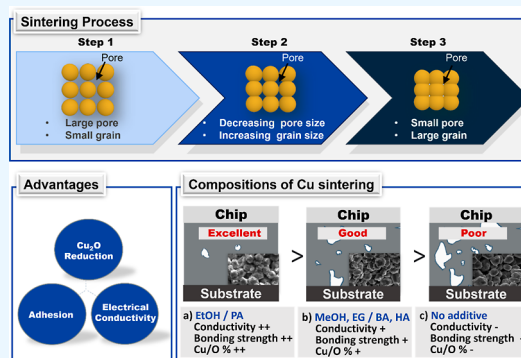


Article Recommendations



Supporting Information

ABSTRACT: Devices in the developing semiconductor market require high density, high integration, and detailed processing. Conventional wire bonding is inappropriate for fine-sized devices, and connected wires can be damaged by heat generation and external physical impact. Soldering is also used in advanced packaging technologies. However, disturbances and overhead joints can occur during bonding. Thus, sintering has been extensively utilized to overcome these drawbacks. Sintering pastes are pressurized and bonded, resulting in stable bonding during sintering. In this study, the composition of the Cu sintering material was examined using diverse additives and solvents. We manufactured sintering materials comprising Cu (1 μm), a solvent [methanol (MeOH), ethanol (EtOH), or ethylene glycol (EG)] and an acidic additive (benzoic acid, phthalic acid, or hexanoic acid). After the sintering process, the mechanical and electrical characteristics were compared to determine the optimal composition and bonding conditions. The optimum ratios between the acid and solvent were 4:6 (MeOH and EtOH) and 2:8 (EG) due to the high viscosity and effective long-term storage. All samples using EtOH as the solvent exhibited the highest sintering performances. The aromatic and carboxylic groups substantially improved the sintering performance and increased the electrical conductivity. Based on the $\text{O}^{1s}/\text{Cu}^{2p}$ ratio (2.23%), the best sintering composition was EtOH/PA, which showed the highest electrical conductivity (ca. 10^4 S/m) and strength (34.0 MPa). The sintering process using various additives and solvents can be helpful to determine the sintering conditions while maintaining the electrical properties.



1. INTRODUCTION

Micro- and nanometal particles have been widely used in diverse applications, such as interconnections and conductive inks.^{1,2} In particular, Ag and Cu have been used as sintering materials for sintering interconnections (Figure 1) owing to

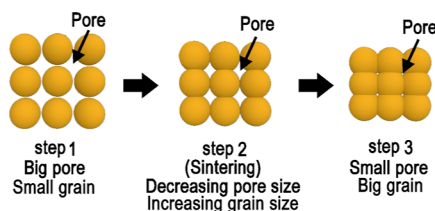


Figure 1. Schematic illustration of the sintering process.

their high electrical and thermal conductivities.^{3,4} Silver was more widely used in sintering applications at the beginning owing to the characteristics of noble metals.^{5,6} However, the high cost of Ag materials impedes their commercialization and large-scale applications. Cu-based bonding (sintering) materials feature their high electrical and thermal conductivities at a low cost.^{7,8} Furthermore, Cu exhibits better anti-ionic migration characteristics than Ag.⁹ However, Cu features a thermodynamically favorable copper oxide (passivation layer)

formation in ambient environments.¹⁰ The passivation layer commonly elevates the sintering temperature due to higher melting point of copper oxides (e.g., CuO: 1330 $^{\circ}\text{C}$) than Cu (1083 $^{\circ}\text{C}$) and reduces the electrical/thermal conductivities.¹⁰ Therefore, the passivation layer on the Cu particle surfaces should be removed and/or prevented. For instance, bimetallic core-shell Cu particles can be utilized to reduce the passivation layer, or reducing agents can be used for maintaining the pristine Cu.^{11,12} The coating (shell) layer reduces the passivation layer; however, a small amount of the passivation layer still exists. Thus, sintering under a reducing atmosphere was found to be the most effective.^{13–15}

Copper can be sintered in oxygen-free or reductive environments, such as hydrogen, nitrogen gas, or gaseous formic acid, to prevent considerable oxidation.^{13–15} Other additives such as acetic, propionic, oxalic, butyric, and citric acids are also used for preventing oxidation.^{16–19} Organic

Received: June 14, 2023

Accepted: September 29, 2023

Published: October 12, 2023



solvents, such as ethylene glycol (EG), are widely utilized to dissolve the additives and disperse the Cu particles in the Cu pastes.^{20,21} The selection and composition of each material are important for the sintering process. However, only a few studies have addressed the sintering materials, although various studies on sintering processing conditions have been conducted. Wide and extensive approaches for the sintering materials are required. In this study, the effects of several additives, solvents, and their combinations on the sintering process were investigated.

2. EXPERIMENTAL SECTION

2.1. Materials. 1 μm sized Cu powders (0809DX, 99%, Sky Spring Nanomaterials, Inc., Houston, TX, USA) were used as electrically conductive particles. Benzoic acid (BA), phthalic acid (1,2-benzenedicarboxylic acid) (PA), and hexanoic acid (HA) were purchased from Tokyo Chemical Industry Co. Methanol (MeOH, Duksan Chemical Co., South Korea), ethanol (EtOH, Samcheon Co., South Korea), and EG (Samcheon Co., South Korea) were used as solvents.

2.2. Fabrication of Cu Sintering Pastes. The carboxylic acid and solvent were mixed in weight ratios of 2:8 or 4:6. The resulting mixture was mixed with excess Cu powder at a weight ratio of 2:8. The final Cu pastes were stirred at room temperature (22–24 °C) for 30 min using a vortex.

2.3. Fabrication of Sintered Cu Pastes. The manufactured Cu pastes (0.4 mL) were injected into molds and preheated without pressure for 10 min before being sealed at 150 °C (for MeOH and EtOH) and 200 °C (for EG) (Figure 2). Subsequently, the Cu pastes were sealed and sintered at 250 °C for 10 min.

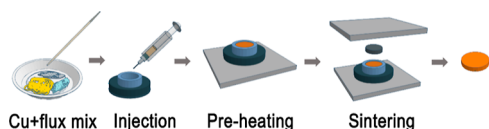


Figure 2. Schematic illustration of the Cu sintering chip fabrication process.

2.4. Characterization. **2.4.1. Thermal Properties.** The thermal properties of Cu pastes were analyzed by using differential scanning calorimetry (DSC; DSC25, TA Instruments Inc., New Castle, DE, USA). Each sample (approximately 3 mg) was sealed between a hermetic Al pan and lid. The sample was heated from –50 to 370 °C at a scanning rate of 10 °C/min under a N₂ atmosphere. The thermal analysis of the Cu pastes was verified using thermogravimetric analysis (TGA; Perkins Elmer Co., Waltham, MA, USA) under a N₂ atmosphere. An average of 1.5 mg of samples was heated from 50 to 500 °C at a heating rate of 10 °C/min. Nitrogen gas was purged at a flow rate of 50 mL/min.

2.4.2. Electrical Conductivity. The electrical properties (volume, surface, and specific resistances) of the sintered samples were measured using a four-point probe (MCP-T370, Nittoseiko Analytech Co., Japan). The electrical conductivities were calculated using the volume resistivities.²² The diameter (*D*) and distance between the points (*S*) were 12 and 1.5 mm, respectively. The correction factor (*C*) was determined using the *D* and *S* values. The *D/S* ratio in this study was 8. Therefore, *C*, as determined using the median method, was 3.98, as shown in Table 1.

Table 1. Correction Factor of Circular Shaped Samples for Pin Spacing; $C(D/S)$ ²³

<i>D/S</i>	<i>C(D/S)</i>
3.0	2.2662
4.0	2.9289
5.0	3.3625
7.5	3.9273
10.0	4.1716
15.0	4.3646
20.0	4.4364
40.0	4.5076
∞	4.5324

Reprinted with permission from [Smits, F. M. Measurement of Sheet Resistivities with the Four-Point Probe. *Bell Syst. Tech. J.* 1958, 37 (3), 711–718.]. Copyright 1958 Nokia Corporation and AT&T Archives.

2.4.3. Morphology. The morphology, sintering degree, voids, and organic residues of the sintered Cu were investigated by using scanning electron microscopy (SEM; Apreo, FEI Co., Hillsboro, OR, USA) at a voltage of 10 kV, $\times 100$ magnification, and a current of 6.4 A. The samples were sputtered with Pt prior to analysis. The compositions of the sintered Cu surface and interior were examined by using X-ray photoelectron spectroscopy (XPS; K-Alpha Plus, Thermo Fisher Scientific Co., Waltham, MA, USA). Elemental analysis was performed by comparing the electron binding energies and understanding the chemical stabilities. This binding energy was used to confirm the component ratio of the sintering chips, such as Cu 2p and C 1s. The Cu, C, and O ratios were determined based on their atomic percentages. The components were detected after being etched for 60 s. The peaks at 285.0, 531.0, and 932.6 eV were ascribed to C 1s, O 1s, and Cu 2p_{3/2}, respectively. An ion beam-based etching process was performed 10 times on the specimen surfaces to analyze the internal component ratio of the chips, and each etching cycle lasted 60 s. The compositions (Cu, C, and O) were determined after each etching cycle. The organic residues and elemental concentrations were determined using X-ray diffraction (XRD, ARL Equinox 3000, Thermo Fisher Scientific Inc., Waltham, MA, USA), which was performed in the bulk mode at the Center for Advanced Materials Analysis. Cu *K* α radiation was applied ($\lambda = 0.1540$ nm) at a voltage of 40 kV and a current of 30 mA.

2.4.4. Mechanical Properties. The mechanical properties of the sintered Cu were investigated using tensile lap shear strength tests with a universal testing machine (UTM; DUT-500CM, Daekyung Engineering, South Korea). Figure 3 describes the stencil-printing, sintering, and tensile lap shear strength tests. The Cu paste was stencil-printed with dimensions of 20 \times 20 \times 0.2 mm on the bottom Cu substrate. Prior to sintering, the sample was preheated without pressure for 5 min at 150 and 200 °C for MeOH and EtOH, and EG, respectively. The topmost Cu substrate was placed on the preheated Cu paste. Subsequently, the sample was sintered at 250 °C for 10 min. The sintered samples were cooled to room temperature for bonding tests. The velocity of the tensile mode was 125 mm/min during the tensile lap shear strength tests.

3. RESULTS AND DISCUSSION

3.1. Miscibility and Stability of Cu Pastes. Metal oxides can be removed by rosin, organic/inorganic acids, and

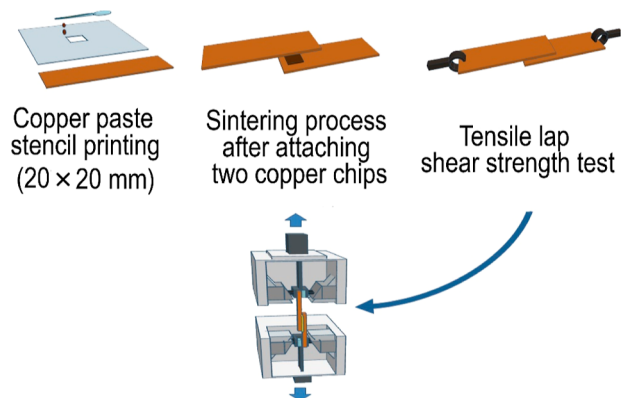


Figure 3. Cu paste stencil printing, sintering, and tensile lap shear strength testing using an UTM.

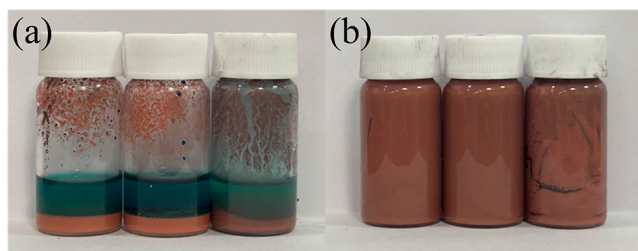


Figure 4. Mixing methods for Cu paste: (a) Cu powders and additives were mixed first, and then the solvent was added (Cu/Add-Sol). (b) Solvents and additives were mixed first, and then, Cu powders were added (Sol/Add-Cu).

Table 2. Ratios and Mass of Each Material in Various Mixtures

additive/solvent/Cu
0:10:40: (0 g/2.5 g/10.0 g)
2:8: 40: (0.5 g/2.0 g/10.0 g)
4:6: 40: (1.0 g/1.5 g/10.0 g)
6:4: 40: (1.5 g/1.0 g/10.0 g)
8:2: 40: (2.0 g/0.5 g/10.0 g)

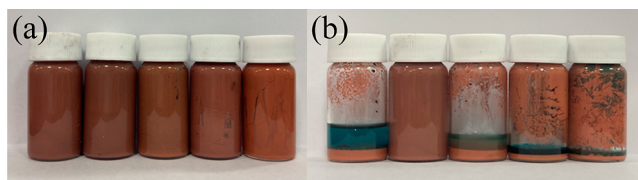


Figure 5. Cu pastes with different compositions of additive and solvent (EtOH) (0:10, 2:8, 4:6, 6:4, and 8:2 from left to right): (a) immediately after fabrication and (b) 24 h after fabrication.

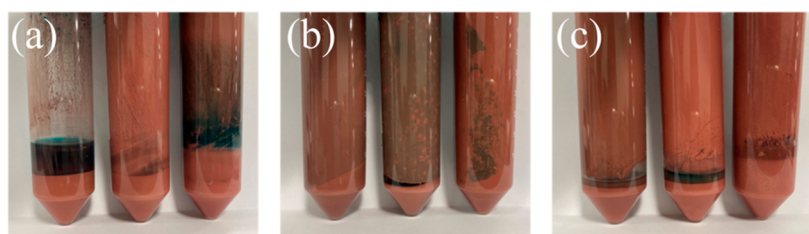


Figure 6. Cu pastes with different additives and solvents were prepared 24 h after fabrication. From left to right for each panel, MeOH, EtOH, and EG. Additive: (a) HA, (b) PA, and (c) BA.

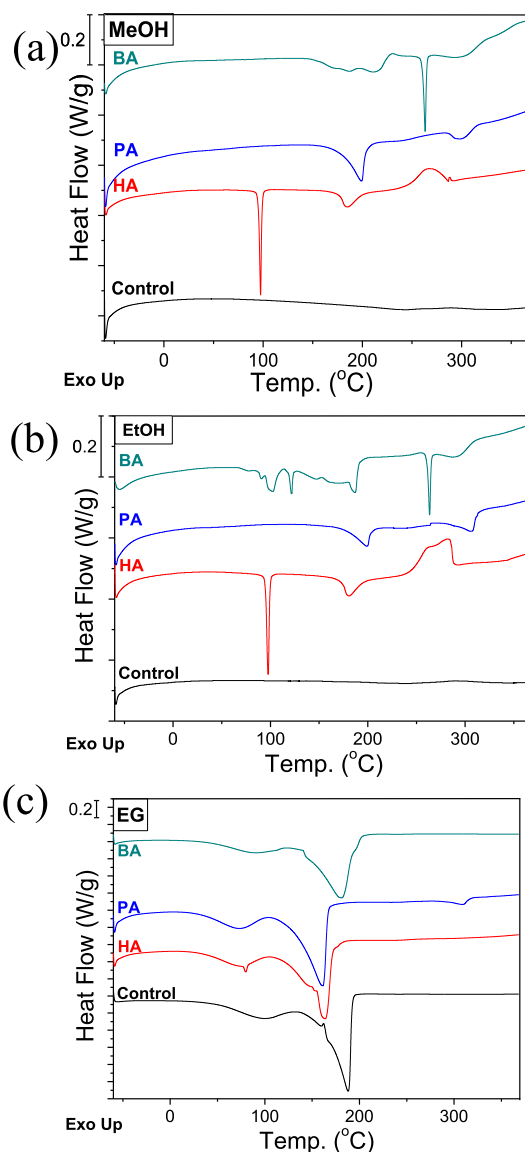


Figure 7. DSC thermograms of Cu sintering pastes composed of HA, PA, or BA with various solvents: (a) EtOH, (b) MeOH, and (c) EG. “Control” indicates the Cu sintering paste containing no activator but a solvent.

hydroxyl and amine groups. Among them, the carboxylic acids are commonly used for removing and preventing the metal oxides.²⁴ The HA, BA, and PA were used as activators in this study. HA and BA were compared to investigate the effect of an aromatic and an aliphatic group on the sintering performance. The impact of the acidic concentration (mono-

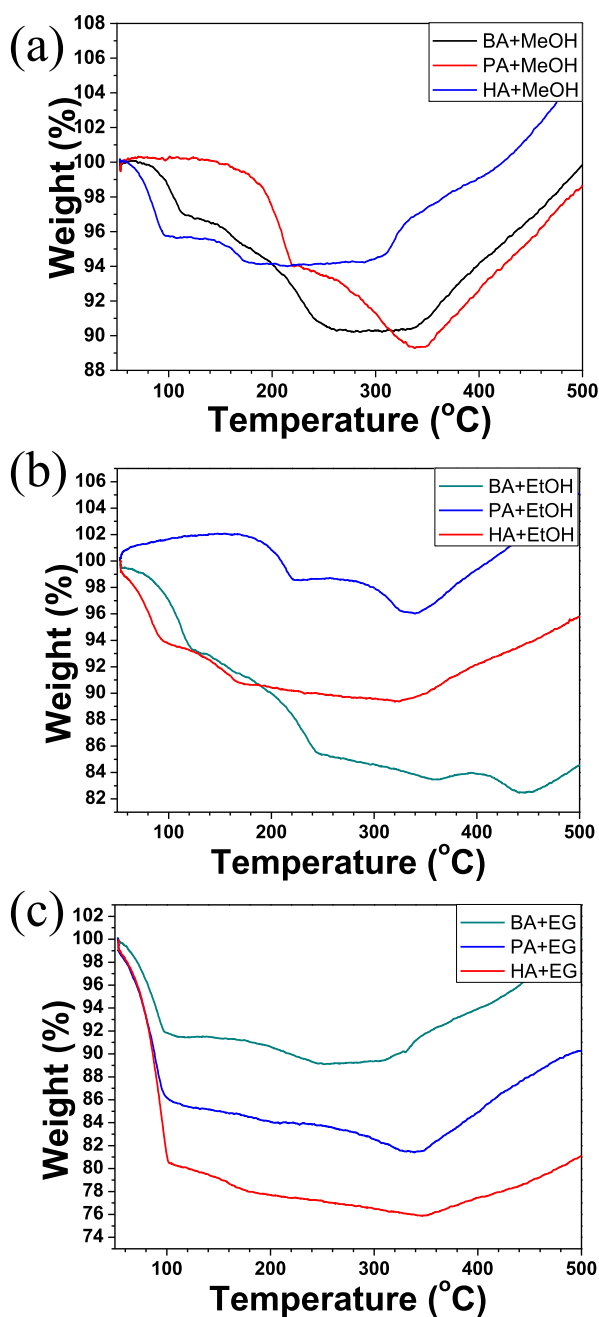


Figure 8. TGA results of the Cu sintering pastes composed of HA, PA, or BA with various solvents: (a) EtOH, (b) MeOH, and (c) EG.

vs diacid) on the sintering performance was investigated using BA and PA. MeOH, EtOH, and EG were used as solvents. MeOH and EtOH were compared to examine the effect of aliphatic chain length of the solvent, whereas EtOH and EG were compared to study the influence of hydroxyl concentration (mono- vs dihydroxyl) of the solvent.

The dispersion and separation of the mixtures at various ratios prior to sintering were examined. Two different mixing methods were investigated and compared. In the first method (Cu/Add-Sol), Cu powders and an additive were mixed, and the mixture was subsequently mixed with a solvent (Figure 4a). In the second method (Sol/Add-Cu), a solvent and an additive were mixed, and the intermediate mixture was subsequently mixed with Cu powder (Figure 4b). The solution fabricated using Cu/Add-Sol exhibited phase separation because of the

oxidation–reduction reaction between the Cu powder and the additive, whereas Sol/Add-Cu did not exhibit phase separation, presenting a homogeneous dispersion. This indicates that the mixing procedure is important for dispersion. Therefore, the sintering materials for all samples in this study were mixed according to the Sol/Add-Cu method. Furthermore, the effect of the composition (Table 2) on phase separation was examined.

Figure 5a,b shows the mixtures containing an activator, solvent, and Cu powder immediately and 24 h after Cu paste fabrication, respectively. The Cu pastes of all compositions were homogeneously mixed immediately after fabrication, whereas most Cu pastes, except for that with the composition ratio of 2:8, were phase-separated 24 h after fabrication. The Cu powder was heterogeneously dispersed in the solvent in the absence of additives. The incorporation of a small concentration of the additive resulted in good dispersion. The dispersion decreased as a function of the additive content. Excessive concentrations of the additive deteriorated the dispersion. The miscibility and stability of various compositions were examined to determine the optimal composition. To avoid precipitation, the optimal ratios between the acid and MeOH or EtOH and between the acid and EG were 4:6 and 2:8, respectively.

The mixtures containing EtOH as a solvent exhibited less phase separation among the three solvents, whereas those comprising MeOH or EG exhibited phase separation with a green color, which may have been caused by oxidation among the Cu pastes, solvent, and oxygen in air (Figure 6).

3.2. Thermal Properties of Cu Paste. Thermal properties of composites are routinely investigated using DSC and TGA.^{25,26} The thermal properties of the Cu sintering pastes were examined by using DSC prior to sintering. The type of solvent and additive used influenced the DSC thermograms and endothermic/exothermic peaks. The unsintered pastes were investigated to determine their preheating and sintering temperatures. The additives should induce neat Cu without Cu oxide layers prior to solvent evaporation. Figure 7a–c shows the DSC thermograms of Cu sintering pastes containing MeOH, EtOH, and EG, respectively. The purity of the Cu should be as high as possible to achieve excellent electrical and mechanical properties after sintering. The additives and solvents should be removed after eliminating Cu oxide layers. The sintering processes involving preheating and heating were selected according to their thermal and sintering characteristics. EtOH and MeOH evaporated at 60–80 °C, whereas EG evaporated at approximately 200 °C. Thus, the preheating temperatures for EtOH/MeOH and EG should be higher than 80 and 200 °C, respectively.

All Cu pastes exhibited broad exothermic peaks above 300 °C owing to the oxidation of Cu. The endothermic peaks at approximately 200 and 250 °C for BA-MeOH and BA-EtOH samples were attributed to the melting and boiling points of BA, respectively, whereas the endothermic peaks at approximately 200 and 300 °C for PA-MeOH and PA-EtOH were attributed to the melting and boiling points of PA, respectively. The endothermic peak at approximately 200 °C for HA-MeOH and HA-EtOH was attributed to the boiling point of HA. All samples containing EG did not exhibit any peak above the boiling point of EG at approximately 200 °C, below which the activators are still dissolved in EG, thereby exhibiting no peak or overlapped peaks.

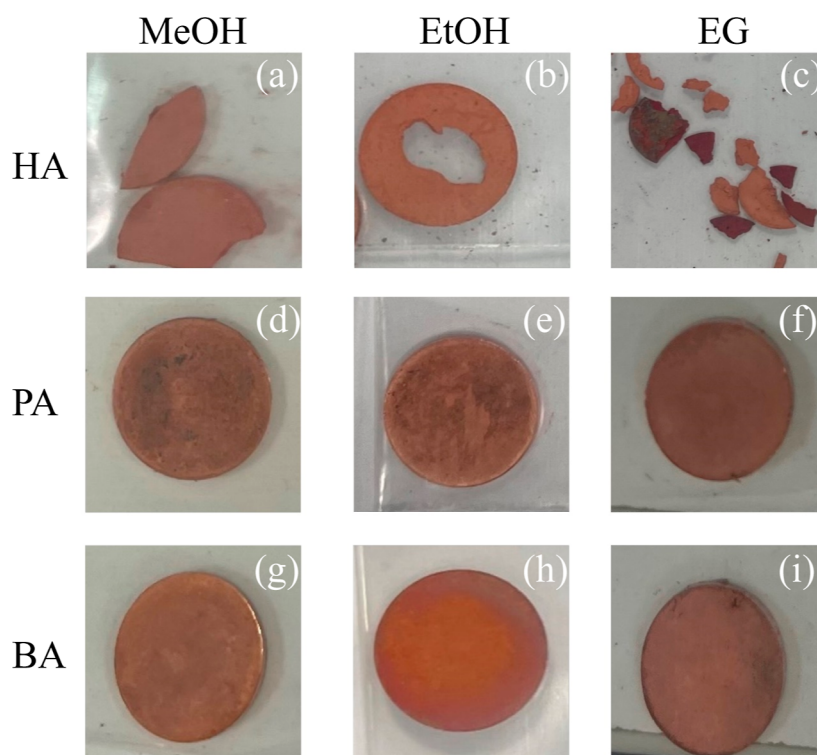


Figure 9. Photographic images of fabricated sintered Cu bonding chips. MeOH, EtOH, and EG were used as solvents. Sintered chips were made using HA (a–c), PA (d–f), and BA (g–i) as additives.

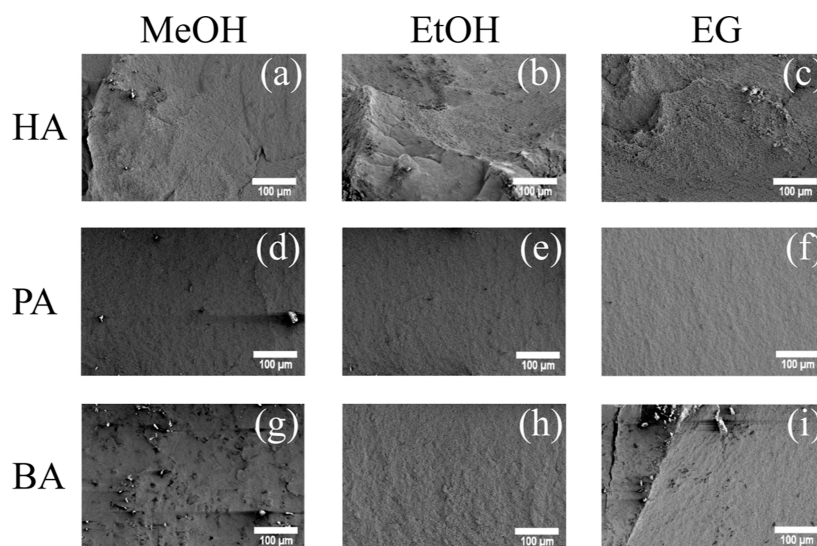


Figure 10. SEM images of fractured surfaces of sintered Cu bonding chips with various activators. Solvent: (a,d,g) MeOH, (b,e,h) EtOH, and (c,f,i) EG. Activator: (a–c) HA, (d–f) PA, and (g–i) BA.

TGA was utilized to confirm the oxidation of Cu with an increasing temperature. The initial weight loss was ascribed to boiling of the organic compounds in all samples. The initial temperatures for Cu-oxidation for MeOH, EtOH, and EG were approximately 320, 340, and 300 °C, respectively. This oxidation corresponded to the DSC results. Thus, the Cu sintering pastes containing EtOH exhibited a somewhat higher thermal stability. The sintering process should be completed below the initial temperatures of Cu-oxidation. Thus, 250 °C was selected as the sintering temperature (Figure 8).²⁷

3.3. Morphology of Sintered Cu Chips. The Cu pastes were sintered and transitioned to Cu bonding chips, the

mechanism of which can be utilized by applying unsintered Cu pastes for sintering to lead to bonding between the topmost chips (or substrates) and the bottom substrates in semiconductor packaging applications, as shown in Figure 9. The activator is homogeneously dissolved and dispersed within the solvent, facilitating the removal of the metal oxide species. Subsequent to the activator-solvent system's involvement, both entities undergo evaporation during the sintering process. The optimization of timing and procedural steps significantly influences the sintering performance outcome. Sintered Cu chips were successfully fabricated using BA and PA, regardless of the solvent type. In contrast, the Cu chip fabricated using

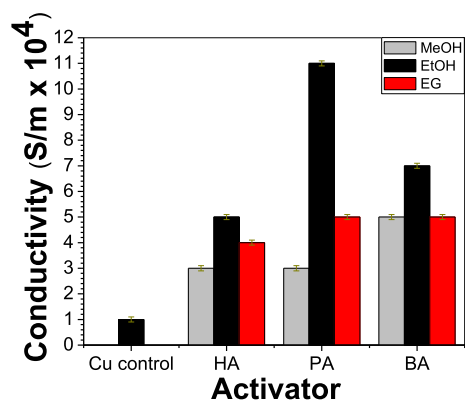


Figure 11. Electrical conductivities of the sintered Cu bonding chip samples with various solvents and activators.

Table 3. Atomic Ratios [O^{1s}/Cu^{2p} (%)] of Sintered Cu Bonding Chips with Various Solvents as Determined Using XPS

	no activator	BA	PA	HA
MeOH	23.4	3.1	5.4	8.0
EtOH	23.4	5.2	2.2	9.1
EG	23.4	5.2	18.5	23.1

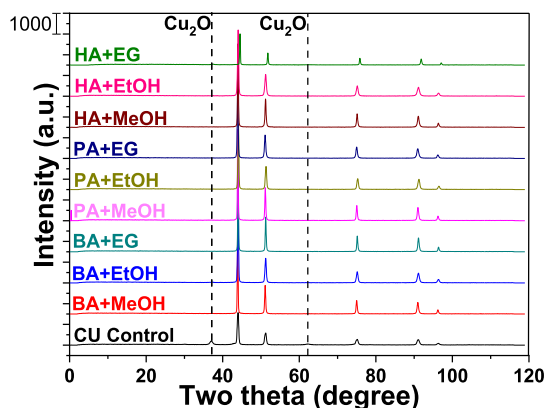


Figure 12. XRD spectra of sintered Cu bonding chips with various solvents and additives.

HA was broken, and the quality of the chips was poor, possibly because of the high viscosity and organic residues. The Cu oxide layers were barely removed, and the solvent evaporated insufficiently during the sintering process. The fractured surfaces of the sintered Cu bonding chips were investigated by using SEM, as shown in Figure 10. The incorporation of an aromatic additive (BA), as compared to HA (aliphatic), into the pastes produced more uniform bonding in the Cu chip. In the case of identical aromatic compounds, the Cu chip consisting of a diacid activator (PA), as compared to a monoacid activator (BA), had slightly neater morphology owing to higher carboxylic concentration of PA. Thus, the combination of aromatic and diacidic moieties led to the excellent sintering performance. The influence of the solvent type on the sintering quality was also examined (Figure 10). The sintering quality obtained using EtOH (moderate boiling point) was superior to that obtained using MeOH (low boiling point) or EG (high boiling point). MeOH evaporated rapidly, thereby impeding the sintering process, whereas EG evaporated considerably slowly and thus remained in the

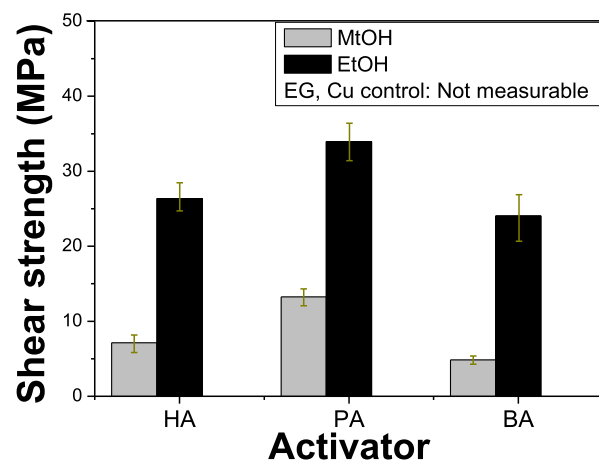


Figure 13. Tensile lap shear strengths after stencil printing and sintering processes as determined using UTM. “EG, Cu control: Not measurable” indicates that sintering pastes containing EG as a solvent or no solvent failed to fabricate the shear test specimens after sintering.

sintered Cu chip. Moreover, the aliphatic chain length and hydroxyl concentration of the solvents may have affected the sintering performance.

3.4. Electrical Properties of Sintered Cu Chips. The electrical properties of sintered Cu bonding chips are the most crucial for the sintering performance in that the primary purpose of sintering is to provide electrical paths between the topmost chips (or substrates) and the bottom substrates. Figure 11 compares the electrical conductivities of the sintered Cu bonding chips prepared by using various solvents and activators. The sintered Cu bonding chips using MeOH and EG without activators were not obtained owing to poor reduction of copper oxides. The electrical conductivities of the sintered Cu bonding chips containing BA as an activator and diverse solvents (MeOH, EtOH, and EG) were 5×10^4 , 7×10^4 , and 5×10^4 S/m, respectively. The electrical conductivities, regardless of the activator, were the highest when EtOH was used as the solvent. The boiling point and ratio between the hydroxyl and aliphatic groups of the solvent influenced the sintering performance and electrical properties, as discussed in the morphological studies (Section 3.3). Hydroxyl moieties typically aid in the prevention of metal oxidation. The incorporation of PA into the Cu sintering pastes with EtOH considerably increased the electrical conductivity to 11×10^4 S/m. This trend is attributed to the morphological results. Each aromatic and carboxylic moiety prevented oxidation and enhanced the sintering performance, thereby increasing the electrical conductivity. The combination of PA and EtOH resulted in excellent sintering performance and electrical conductivity.

3.5. Atomic Analysis by XPS. Table 3 lists the atomic ratios (O^{1s}/Cu^{2p} × 100%) of the sintered Cu bonding chips with various solvents (MeOH, EtOH, and EG) based on the XPS results shown in Figure 12. The atomic ratio of the sintered Cu chip without additives was 23.4%, whereas the incorporation of additives considerably reduced the atomic ratio. For instance, in the case of the MeOH solvent, the atomic ratios of BA, PA, and HA were 3.1, 5.4, and 8.0%, respectively. When MeOH and EtOH were used as solvents, the atomic ratios were lower than those of EG because of their low vapor pressures. Thus, the solvent was retained. The

combination of PA and EtOH exhibited the lowest ratio, indicating the highest sintering performance owing to the higher carboxylic concentration and synergy; PA was soluble and remained in the solvent for longer upon heating, and the solvent was subsequently completely removed prior to sintering.

XRD was used to further demonstrate the removal of the Cu oxide layers. The peaks at $2\theta = 42, 50, 75, 90,$ and 95° were ascribed to the Cu component, whereas those at $2\theta = 38$ and 62° contributed to Cu_2O . The Cu_2O peaks substantially decreased and were hardly visible due to the combination of the solvent and additive. These findings represent that sintering almost completely eliminated the Cu oxide layers on the Cu particles.

3.6. Mechanical Properties of Sintered Cu Chips.

Sintered Cu chips require robustness and electrical properties. UTM is a powerful tool for various mechanical properties.^{28,28,29} Figure 13 shows the shear strength of the sintered Cu chip samples with different activators and solvents. The PA-incorporated sintered Cu samples exhibited the highest mechanical properties regardless of the solvent type, similar to the electrical conductivity results. The sintered Cu chip using PA and EtOH exhibited the highest tensile lap shear strength of 34.0 MPa, which was caused by the higher carboxylic concentration that led to a uniform bonding quality.³⁰ However, the HA-infiltrated sintered Cu sample exhibited slightly higher mechanical properties than the BA-embedded samples, which contradicts the electrical and morphological results. This is because the BA in the solution tends to crystallize when exposed to air (Figure S1). The crystallized parts of the BA contributed to the lower robustness than anticipated. The effect of the solvent type on the mechanical properties of the sintered Cu bonding chips was investigated, which revealed that all of the samples exhibited inconsistent mechanical properties. The tensile lap shear strength of the sintered Cu chip using PA and MeOH was 13.3 MPa, which was lower than that using PA and EtOH. The mechanical properties of the sintered Cu chips using EG as a solvent could not be measured owing to poor robustness.

4. CONCLUSIONS

Sintering was performed by using Cu sintering pastes at elevated temperatures and pressures. We examined the effects of the activator and solvent on the sintering performance, including electrical, mechanical, elemental, and morphological properties of the sintered Cu bonding chips, which were examined. The activators used were HA, BA, and PA. The effect of the presence or absence of an aromatic ring on the sintering performance was compared using HA and BA. The impact of the acidic concentration on the sintering performance was investigated using BA and PA. In terms of the solvent, MeOH and EtOH were compared to examine the effect of the aliphatic chain length of the solvent, whereas EtOH and EG were compared to study the influence of the hydroxyl concentration of solvent. The combination of PA and EtOH as an activator and solvent achieved the highest sintering performance with high purity. Correlations between the sintering processing conditions (temperature, time, pressure, and cycling steps) and the sintering materials, including solvents and activators, should be further explored in future studies. The sintering process using various activators and solvents can be helpful to determine the sintering conditions and maintain the electrical properties.

■ ASSOCIATED CONTENT

Supporting Information

The Supporting Information is available free of charge at <https://pubs.acs.org/doi/10.1021/acsomega.3c04245>.

Photographic images taken immediately after mixing the solvent and BA, 5 min after mixing in air, and immediately after Cu powders added to the mixture (solvent/acid) (MtOH, EtOH, and EG) (PDF)

■ AUTHOR INFORMATION

Corresponding Author

Keon-Soo Jang – Department of Polymer Engineering, School of Chemical and Materials Engineering, The University of Suwon, Hwaseong, Gyeonggi-do 18323, Republic of Korea; orcid.org/0000-0002-0883-2683; Email: ksjang@suwon.ac.kr

Authors

Seungyeon Lee – Department of Polymer Engineering, School of Chemical and Materials Engineering, The University of Suwon, Hwaseong, Gyeonggi-do 18323, Republic of Korea
Seong-ju Han – Department of Polymer Engineering, School of Chemical and Materials Engineering, The University of Suwon, Hwaseong, Gyeonggi-do 18323, Republic of Korea
Yongjune Kim – Department of Electrical Engineering, The University of Suwon, Hwaseong, Gyeonggi-do 18323, Republic of Korea

Complete contact information is available at: <https://pubs.acs.org/10.1021/acsomega.3c04245>

Author Contributions

[§]S.L. and S.H. contributed equally and are co-first authors.

Notes

The authors declare no competing financial interest.

■ ACKNOWLEDGMENTS

This work was supported by the Technology Innovation Program (or Industrial Strategic Technology Development Program-Material Components Technology Development Program) (no. 20011433, Extremely cold-resistant antivibration elastomer with EPDM) funded by the Ministry of Trade, Industry & Energy (MOTIE, Korea). This work was supported by the National Research Foundation of Korea (NRF) grant funded by the Korea government (MSIT) (no. 2021R1G1A1011525, Rapid low-temperature curing of thermoset resins via microwave). This work was supported by the Technology Innovation Program (or Industrial Strategic Technology Development Program-Nano fusion innovative product technology development) (no. 20014475, Antifog nanocomposite-based head lamp with <10% of low moisture adsorption in surface area) funded By the Ministry of Trade, Industry & Energy (MOTIE, Korea). This work was supported by the Technology Innovation Program (or Industrial Strategic Technology Development Program-Automobile industry technology development) (20015803, High performance composite-based battery pack case for electric vehicles via hybrid structure and weight lightening technology) funded By the Ministry of Trade, Industry & Energy (MOTIE, Korea). This work was supported by the Technology development Program (Antistatic extrudable carbon nanotube/polymer composites with 10^6 to 10^8 ohm/sq of surface resistance for display tray: S3111196) funded by the Ministry of SMEs and Startups

(MSS, Korea). This work was supported by the INNOPOLIS Foundation grant funded by the Korea government (MSIT) (Development of sintered Cu bonding material with Pb-free for power semiconductor module: 2021-DD-RD-0385-01). This research was supported by Research and Business Development Program through the Korea Institute for Advancement of Technology (KIAT) funded by the Ministry of Trade, Industry and Energy (MOTIE) (Development of one step black epoxy bonding film for micro LED display, grant number: P0018198). This work was supported by the Technological Innovation R&D Program (Development of metal–polymer heterojunction bonding technology using metal surface treatment and compatibilizing agents for lightweighting: S3236143) funded by the Ministry of SMEs and Startups (MSS, Korea). This work was supported by ITECH R&D program of MOTIE/KEIT (project no. 20024384, Development of a battery housing cover using high orientation composite material with a fiber content of 40% and using recycled fibers and engineering plastics). This study was supported by the research grant of The University of Suwon in 2022. This research was also supported by Advanced Materials Analysis Center, The University of Suwon.

REFERENCES

- (1) Kim, S. J.; Stach, E. A.; Handwerker, C. A. Fabrication of Conductive Interconnects by Ag Migration in Cu-Ag Core-Shell Nanoparticles. *Appl. Phys. Lett.* **2010**, *96* (14), 144101.
- (2) Li, W.; Sun, Q.; Li, L.; Jiu, J.; Liu, X.-Y.; Kanehara, M.; Minari, T.; Sugauma, K. The Rise of Conductive Copper Inks: Challenges and Perspectives. *Appl. Mater. Today* **2020**, *18*, 100451.
- (3) Chen, T. F.; Siow, K. S. Comparing the Mechanical and Thermal-Electrical Properties of Sintered Copper (Cu) and Sintered Silver (Ag) Joints. *J. Alloys Compd.* **2021**, *866*, 158783.
- (4) Siow, K. S.; Chua, S. T.; Beake, B. D.; Zuruzi, A. S. Influence of Sintering Environment on Silver Sintered on Copper Substrate. *J. Mater. Sci. Mater. Electron.* **2019**, *30* (6), 6212–6223.
- (5) Chen, C.; Sugauma, K. Microstructure and Mechanical Properties of Sintered Ag Particles with Flake and Spherical Shape from Nano to Micro Size. *Mater. Des.* **2019**, *162*, 311–321.
- (6) Chen, C.; Yeom, J.; Choe, C.; Liu, G.; Gao, Y.; Zhang, Z.; Zhang, B.; Kim, D.; Sugauma, K. Necking growth and mechanical properties of sintered Ag particles with different shapes under air and N₂ atmosphere. *J. Mater. Sci.* **2019**, *54* (20), 13344–13357.
- (7) Peng, Y.; Mou, Y.; Liu, J.; Chen, M. Fabrication of High-Strength Cu-Cu Joint by Low-Temperature Sintering Micron-Nano Cu Composite Paste. *J. Mater. Sci. Mater. Electron.* **2020**, *31* (11), 8456–8463.
- (8) Akbarpour, M. R.; Mousa Mirabad, H.; Khalili Azar, M.; Kakaei, K.; Kim, H. S. Synergistic Role of Carbon Nanotube and SiCn Reinforcements on Mechanical Properties and Corrosion Behavior of Cu-Based Nanocomposite Developed by Flake Powder Metallurgy and Spark Plasma Sintering Process. *Mater. Sci. Eng., A* **2020**, *786*, 139395.
- (9) Liu, Y.; Yu, Y.; Lin, S.; Chiu, S.-J. Electromigration Effect upon Single- and Two-Phase Ag-Cu Alloy Strips: An in Situ Study. *Scr. Mater.* **2019**, *173*, 134–138.
- (10) Li, J.; Li, X.; Wang, L.; Mei, Y.-H.; Lu, G.-Q. A Novel Multiscale Silver Paste for Die Bonding on Bare Copper by Low-Temperature Pressure-Free Sintering in Air. *Mater. Des.* **2018**, *140*, 64–72.
- (11) Zhang, W.; Zhou, Y.; Ding, Y.; Song, L.; Yuan, Q.; Zhao, W.; Xu, C.; Wei, J.; Li, M.; Ji, H. Sintering Mechanism of Size-Controllable Cu-Ag Core-Shell Nanoparticles for Flexible Conductive Film with High Conductivity, Antioxidation, and Electrochemical Migration Resistance. *Appl. Surf. Sci.* **2022**, *586*, 152691.
- (12) Dai, X.; Xu, W.; Zhang, T.; Shi, H.; Wang, T. Room Temperature Sintering of Cu-Ag Core-Shell Nanoparticles Conductive Inks for Printed Electronics. *Chem. Eng. J.* **2019**, *364*, 310–319.
- (13) Yang, W.; Wan, J.; Wu, C.; Xie, C.; Huang, Z. Sintering of Mixed CuAg Nanoparticles Pretreated by Formic Acid Vapor for CuCu Low Temperature Bonding. *Microelectron. Reliab.* **2023**, *141*, 114890.
- (14) Yonezawa, T.; Tsukamoto, H.; Yong, Y.; Nguyen, M. T.; Matsubara, M. Low Temperature Sintering Process of Copper Fine Particles under Nitrogen Gas Flow with Cu 2+ -Alkanolamine Metallacycle Compounds for Electrically Conductive Layer Formation. *RSC Adv.* **2016**, *6* (15), 12048–12052.
- (15) Li, J. J.; Cheng, C. L.; Shi, T. L.; Fan, J. H.; Yu, X.; Cheng, S. Y.; Liao, G. L.; Tang, Z. R. Surface Effect Induced Cu-Cu Bonding by Cu Nanosolder Paste. *Mater. Lett.* **2016**, *184*, 193–196.
- (16) Young, K.; Chowdhury, R.; Jang, S. Copper Nanoparticle Conductive Patterns Fabricated by Thermal Sintering Using Carboxylic Acid Vapors and Their Application for Radio-Frequency Identification Antennas. *Appl. Phys. A: Mater. Sci. Process.* **2023**, *129* (3), 207.
- (17) Kwon, J.; Cho, H.; Suh, Y. D.; Lee, J.; Lee, H.; Jung, J.; Kim, D.; Lee, D.; Hong, S.; Ko, S. H. Flexible and Transparent Cu Electronics by Low-Temperature Acid-Assisted Laser Processing of Cu Nanoparticles. *Adv. Mater. Technol.* **2017**, *2* (2), 1600222.
- (18) Woo, K.; Kim, Y.; Lee, B.; Kim, J.; Moon, J. Effect of Carboxylic Acid on Sintering of Inkjet-Printed Copper Nanoparticulate Films. *ACS Appl. Mater. Interfaces* **2011**, *3* (7), 2377–2382.
- (19) Wang, B.-Y.; Yoo, T.-H.; Song, Y.-W.; Lim, D.-S.; Oh, Y.-J. Cu Ion Ink for a Flexible Substrate and Highly Conductive Patterning by Intensive Pulsed Light Sintering. *ACS Appl. Mater. Interfaces* **2013**, *5* (10), 4113–4119.
- (20) Zuo, Y.; Carter-Searjeant, S.; Green, M.; Mills, L.; Mannan, S. H. High Bond Strength Cu Joints Fabricated by Rapid and Pressureless in Situ Reduction-Sintering of Cu Nanoparticles. *Mater. Lett.* **2020**, *276*, 128260.
- (21) Yu, X.; Li, J.; Shi, T.; Cheng, C.; Liao, G.; Fan, J.; Li, T.; Tang, Z. A Green Approach of Synthesizing of Cu-Ag Core-Shell Nanoparticles and Their Sintering Behavior for Printed Electronics. *J. Alloys Compd.* **2017**, *724*, 365–372.
- (22) Schomer, D. L.; Silva, F. L. da. *Niedermeyer's Electroencephalography: Basic Principles, Clinical Applications, and Related Fields*; Lippincott Williams & Wilkins, 2012.
- (23) Smits, F. M. Measurement of Sheet Resistivities with the Four-Point Probe. *Bell Syst. Technol. J.* **1958**, *37* (3), 711–718.
- (24) Lee, B.-Y.; Lee, D.-H.; Jang, K.-S. Impact Modifiers and Compatibilizers for Versatile Epoxy-Based Adhesive Films with Curing and Deoxidizing Capabilities. *Polymers* **2021**, *13* (7), 1129.
- (25) Park, C.; Kim, C. B. Efficient Carbonization of ABS Rubber via Iodine Doping. *Elastomers Compos.* **2022**, *57* (1), 9–12.
- (26) Lee, E. K.; Han, S. Y. Synthesis and Characterization of the Ag-Doped TiO₂. *Elastomers Compos.* **2022**, *57* (1), 1–8.
- (27) Joo, S.; Baldwin, D. F. Performance of Silver Nano Particles as an Electronics Packaging Interconnects Material. *2007 Proceedings 57th Electronic Components and Technology Conference; IEEE, 2007*; pp 219–226.
- (28) Choi, J.; Lim, J.; Han, S.; Kim, H.; Choi, H. J.; Seo, Y. How to Resolve the Trade-off between Performance and Long-Term Stability of Magnetorheological Fluids. *Korea-Aust. Rheol. J.* **2022**, *34* (4), 243–290.
- (29) Seo, J.; Kim, W.; Bae, S.; Kim, J. Influence of Loading Procedure of Liquid Butadiene Rubber on Properties of Silica-Filled Tire Tread Compounds. *Elastomers Compos.* **2022**, *57* (4), 129–137.
- (30) Kwon, S.; Lee, T.-I.; Lee, H.-J.; Yoo, S. Improved Sinterability of Micro-Scale Copper Paste with a Reducing Agent. *Mater. Lett.* **2020**, *269*, 127656.